Comparison of Temperature Gradient Model Predictions with Recent Rainfall Trends in the Sahel

GARY K. GREENHUT[1]

National Center for Atmospheric Research,[2] Boulder CO 80307

(Manuscript received 30 November 1978, in final form 21 July 1980)

ABSTRACT

Using the temperature departure data of Angell and Korshover (1978), models relating the movement of the Intertropical Convergence Zone (ITCZ) to hemispheric temperature gradients are compared with rainfall data from the Sahel. The Northern Hemisphere models (Bryson, 1973, 1974; Greenhut, 1977), in general, do not correlate with rainfall. Rainfall is well correlated with meridional temperature gradients taken with constant vertical lapse rate—a result which parallels that of Korff and Flohn (1969) in a study of the motion of the subtropical high. The Southern Hemisphere model relating temperature gradients to ITCZ motion (Kraus, 1977) also is not correlated with rainfall in the Sahel. However, highly significant correlation between rainfall and summer-winter change in the Southern Hemisphere meridional temperature gradient with the latter lagged by 0.5–1 year is evidence that the cross-equatorial transport of energy may be driven to some extent by the movement of the ITCZ in the Northern Hemisphere.

1. Introduction

The tabulation of data on global temperature trends by Angell and Korshover (1978) makes it possible to test various hypotheses which relate horizontal and vertical temperature gradients to the movement of the West African subtropical high-pressure system and the intertropical convergence zone (ITCZ) and to the trends in rainfall in the Sahel. The models to be considered are those of Bryson (1973, 1974, hereafter referred to as model I) and Greenhut (1977). These models are based on earlier work of Smagorinsky (1963) and Flohn (1964, 1965). In addition, the approach taken by Korff and Flohn (1969) will be considered in which model I is used with constant vertical lapse rate. Finally, we test the model of Kraus (1977), referred to as model II, in which Sahelian rainfall trends are related to temperature gradients in the Southern Hemisphere.

In all cases, correlation coefficients are obtained between the model predictions and the Sahel rainfall record. It is found that significant correlation is obtained consistently only in the approach of Korff and Flohn. These authors have already obtained good correlation between the movement of the subtropical high and the equator-pole temperature gradient at the 700–300 mb level. In the present work, their results are extended, implying that significant correlation must also exist between movement of the subtropical high and rainfall in the Sahel.

In the Appendix, a relation between rainfall rate and parameters of the ITCZ is derived from the work of Ilesanmi (1971). The rate of change of rainfall with respect to changes in these parameters is then obtained as a function of latitude.

2. The temperature data

The temperature trend data of Angell and Korshover (1978) are obtained from seasonal deviations from the record mean at each station. They are separated into surface and surface–100 mb data, the latter being pressure interval weighted averages of values at the surface and at the 850, 300 and 100 mb levels. The data are further divided into seven latitude bands: two polar regions (latitudes > 60°), two temperate zones (30–60°), two subtropical zones (10–30°) and an equatorial zone (10°N–10°S). In addition, the data have been divided into Eastern and Western Hemisphere zones, delineated by 0 and 180° longitudes. A final division is into four seasonal values for each year from 1959 to 1976.

Since rainfall in the Sahel occurs mainly in the Northern Hemisphere summer months, only the temperature data for the months April–September will be used in the comparison with predictions of model I and the approach of Korff and Flohn (1969). The locations of stations used to obtain the temperature departures are given in Fig. 1 of Angell and Korshover (1977). J. K. Angell (private com-

[1] Present affiliation: Boundary Layer Dynamics Group, Weather Modification Program Office, NOAA/ERL, Boulder, CO 80303.

[2] The National Center for Atmospheric Research is sponsored by the National Science Foundation.

0027-0644/81/010137-11$06.75

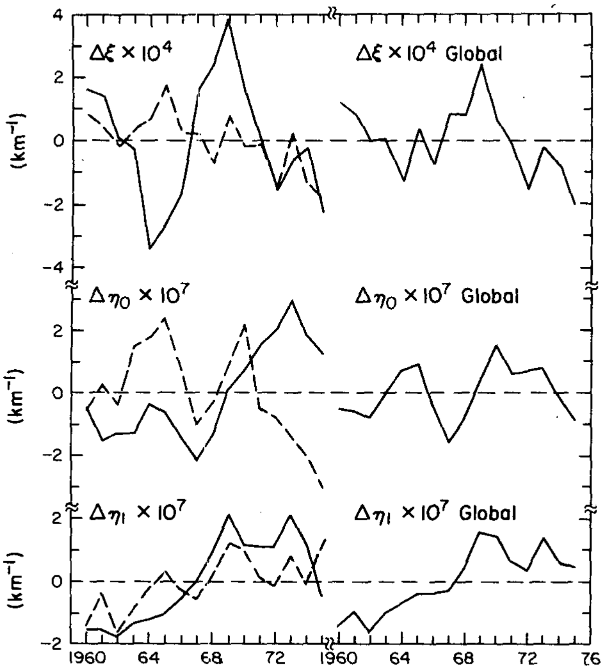

FIG. 1. The parameters $\Delta\xi$, proportional to the change in tropical lapse rate, and $\Delta\eta_0$ and $\Delta\eta_1$, proportional to the change in meridional temperature gradients at the surface and at the ~500 mb level. In the left-hand side of the figure, the dashed and solid curves are for data from the Eastern and Western Hemisphere, respectively.

munication) has provided the unsmoothed and unaveraged data for this analysis. We use temperature deviations obtained from averages of the deviations in the periods April–June and July–September only, instead of full-year averages. This does not significantly change the temperature trends from those obtained by Angell and Korshover (1978) (see their Fig. 6), except in the case of the temperature trends at the surface for the north extratropics where there is a tendency for the temperature deviation to be more negative in the period 1960–63 by ~0.1°C, and more positive in the period 1972–75 by ~0.05°C.

From the unsmoothed data, we obtain four temperature deviations for each year from 1959 through 1976: tropics surface (TT_0), tropics surface–100 mb (TT_1), north extratropics surface (TN_0) and north extratropics surface–100 mb (TN_1). Following Angell and Korshover, the tropics values are obtained by an equal weighted average of north subtropics, equatorial and south subtropics values. The north extratropics values are obtained by a 1–2 weighting of North Polar and north temperate zone values. The results for the four temperature departures are given in Table 1 for the Eastern and Western Hemispheres. Global values for these departures are averages of the Eastern and Western Hemisphere values.

Model I contains the parameters

$$\xi = \frac{\partial(\ln\theta_{PE})}{\partial z}, \quad \eta = -\frac{\partial(\ln\theta_{PE})}{\partial y}, \tag{1}$$

which are related to the vertical lapse rate and meridional temperature gradient, respectively. In Eq. (1), θ_{PE} is the partial equivalent potential temperature and z and y are upward and northward components, respectively. Greenhut (1977) has shown that changes in these quantities are related to changes in temperature gradients such that

TABLE 1. Values of temperature departures from the mean (°C) for tropics surface (TT_0), tropics surface–100 mb (TT_1), north extratropics surface (TN_0) and north extratropics surface–100 mb (TN_1) for the months April–September. [From data supplied by J. K. Angell (private communication).]

	Eastern Hemisphere				Western Hemisphere			
Year	TT_0	TT_1	TN_0	TN_1	TT_0	TT_1	TN_0	TN_1
1959	0.13	0.06	0.85	0.92	0.18	0.31	0.08	0.37
1960	0.18	0.34	−0.47	0	−0.12	0.01	0.10	0.12
1961	0.09	0.18	0.62	0.23	−0.04	−0.03	−0.01	0.49
1962	0.03	−0.10	0.28	0.28	−0.27	−0.18	0.26	−0.10
1963	−0.08	−0.04	−0.40	−0.01	0.09	−0.02	0.22	0.17
1964	−0.05	0.15	−0.54	0	−0.32	−0.38	−0.30	−0.04
1965	−0.20	−0.28	−0.17	−0.19	−0.15	−0.63	−0.15	−0.57
1966	0.11	0.36	−0.53	0.16	−0.16	−0.12	0.05	−0.04
1967	0.20	0.11	0.72	0.24	−0.34	−0.22	0.26	−0.15
1968	−0.23	−0.32	0.80	−0.09	−0.41	−0.30	−0.06	−0.47
1969	0.20	0.28	−0.86	−0.28	0.31	0.50	0.01	0.20
1970	0.03	0.21	−0.18	−0.17	0.05	0.49	−0.14	−0.08
1971	−0.31	−0.58	−0.03	−0.23	−0.10	−0.48	−0.14	−0.11
1972	−0.24	−0.14	0.26	−0.29	0.19	0.11	−0.63	−0.20
1973	0.27	0.19	0.18	−0.02	0.54	0.68	0.09	0.11
1974	−0.27	−0.21	0.44	−0.37	0.16	−0.05	−0.44	−0.21
1975	0.14	−0.08	1.07	0.18	0	0.01	−0.14	0.12
1976	−0.18	−0.33	0.28	−1.17	−0.12	−0.35	−0.28	−0.15

$$\Delta\xi \approx -\frac{2}{T_1} l_\xi, \quad \Delta\eta_i \approx \frac{1}{T_i} l_{\eta_i}, \qquad (2)$$

where the meridional temperature gradient is obtained using the surface (surface–100 mb) data of Table 1 when the subscript i is equal to 0(1). In Eq. (2), $T_0 = 300$ K, the approximate temperature at the surface and $T_1 = 250$ K, the approximate temperature at ~500 mb. The temperature gradients are given by

$$l_\xi = \frac{TT_0 - TT_1}{d_\xi}, \quad l_{\eta_i} = \frac{TT_i - TN_i}{d_\eta}, \qquad (3)$$

where the length scales are $d_\xi = 5$ km and $d_\eta = 6600$ km. The parameter d_ξ is the effective distance between the surface and the surface–100 mb level and d_η is the distance between the tropics and north extratropics, i.e., between 0 and 60°N latitude. When (3) is substituted into (2) and the data in Table 1 are used, seasonal values of $\Delta\xi$, $\Delta\eta_0$ and $\Delta\eta_1$ are obtained for each year. The results are shown in Fig. 1 where 3 year running means have been taken and each time series normalized to zero for the interval 1960–75. These results will be used in the next section to calculate the expected movement of the ITCZ using model I.

In order to test model II, the temperature data of Angell and Korshover (1978) from the Southern Hemisphere are used. Since model II refers specifically to the winter and summer months in the Southern Hemisphere, we shall use the periods January–March (summer) and July–September (winter). The tropics temperature departure values will now be defined as 1–1 averages of the equator and south subtropics data. The data for the south polar sector will be used alone (no averages taken with the adjacent south temperate sector). These definitions correspond closely to the conditions of the hypothesis. In addition, only data for the surface–100 mb level will be used since the model specifically refers to meridional temperature gradients at the 500–700 mb level. From the unsmoothed data supplied by J. K. Angell, four temperature deviations are obtained for each year 1959–76: summer tropics (ST), summer south polar (SS), winter tropics (WT) and winter south polar (WS), each in the Eastern and Western Hemispheres. The results are given in Table 2 and shown in Fig. 2, where 3-year running means have been taken and the results normalized to zero for the period 1960–75.

Model II refers to temperature gradients between the southern tropics and the south polar region. Therefore, we calculate the following quantities using the data of Table 2:

$$\Delta\alpha = ST - SS, \quad \Delta\beta = WT - WS, \qquad (4)$$

where $\Delta\alpha$ and $\Delta\beta$ are the tropics-south polar temperature gradients at the surface–100 mb level in the Southern Hemisphere summer and winter, respectively. These quantities are analogous to $\Delta\eta_1$ in the Northern Hemisphere defined previously. In addition, we calculate

$$\Delta = \Delta\beta - \Delta\alpha, \qquad (5)$$

which is a measure of the change in temperature gradient in the Southern Hemisphere from summer to winter in a given calendar year. The results are shown in Fig. 3 where 3-year running means have

TABLE 2. Values of temperature departures from the mean (°C) for Southern Hemisphere: summer tropics (ST), summer South Polar (SS), winter tropics (WT), and winter South Polar (WS). Summer refers to the months January–March and winter refers to the months July–September. [From data supplied by J. K. Angell (private communication).]

	Eastern Hemisphere				Western Hemisphere			
Year	ST	SS	WT	WS	ST	SS	WT	WS
1959	−0.03	−0.87	−0.23	−0.08	0.12	−0.53	0.37	−0.47
1960	0.19	0.05	0.28	−1.44	0.25	−0.37	0.18	−0.18
1961	0.08	0.08	0.01	0.78	−0.18	0.01	−0.15	−0.49
1962	0.17	−1.58	−0.07	−0.81	−0.17	−0.83	−0.20	−0.10
1963	−0.07	0.12	0.13	−0.78	−0.43	−0.08	0.06	0.52
1964	0.30	0.19	−0.01	1.25	0.05	0.11	−0.82	0.15
1965	−0.72	0.39	−0.33	−0.95	−1.21	0.25	−0.54	0.09
1966	0.31	−0.10	0.31	0.50	−0.02	0.35	−0.33	−0.26
1967	0.02	0.21	0.08	0.84	−0.71	0.88	0.02	0.28
1968	−0.15	−0.57	0.11	0.26	−0.27	0.31	0	−0.83
1969	0.19	0.52	0.20	−0.61	0.20	0.09	0.35	−0.19
1970	0.40	−0.22	0.15	0.36	0.54	−1.08	0.61	0.27
1971	−0.18	0.05	−0.46	−0.08	−0.05	−0.37	−0.46	0.10
1972	−0.34	0.18	0.10	1.06	−0.47	0.11	0.52	0.35
1973	0.63	−0.11	0.12	0.15	1.25	−0.14	0.56	0.49
1974	−0.38	−0.45	−0.15	0.63	−0.01	0.27	0.05	1.57
1975	−0.26	1.16	−0.21	0.18	0.13	0.71	−0.02	−0.31
1976	−0.38	0.33	−0.37	−0.92	−0.17	0.05	−0.22	0.03

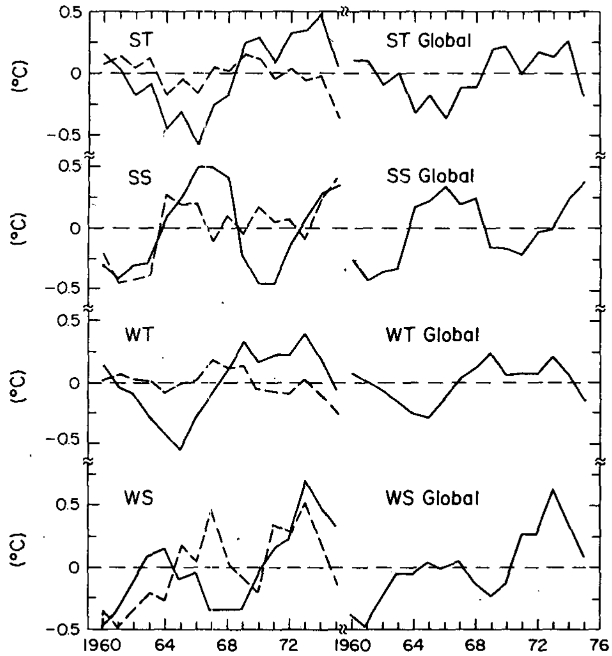

FIG. 2. Southern Hemisphere temperature trends at the ~500 mb level: summer tropics (ST), summer south polar (SS), winter tropics (WT) and winter south polar (WS). Summer refers to the months January through March and winter refers to the months July through September. In the left hand side of the figure, the dashed and solid curves are as in Fig. 1.

been taken and the departures normalized to zero for the period 1960–75. The quantities in Fig. 3 will be used in Section 4 in the discussion of model II.

3. Northern Hemisphere models

Model I (Bryson, 1973, 1974) is based on the equation (Smagorinsky, 1963)

$$\tan\phi = \frac{h}{a}\frac{\xi}{\eta}\,, \tag{6}$$

which, according to Flohn (1964), relates the latitude ϕ of the subtropical high to the scale height h of the atmosphere taken to be 9 km, the radius of the earth a (6371 km), and the parameters ξ and η defined in Eq. (1). Eq. (6) is based on a stability criterion for baroclinic waves developed by Phillips (1954) in a two-level model for meridional circulation. Differentiating both sides of (6) gives the change in ϕ for small changes in ξ and η:

$$\sec^2\phi\Delta\phi = \frac{h}{a}\left(\frac{1}{\eta}\,\Delta\xi - \frac{\xi}{\eta^2}\,\Delta\eta\right)\,. \tag{7}$$

A central value for the latitude of the subtropical high is ~35° (Korff and Flohn, 1969; Beer *et al.*, 1977) and typical values of ξ and η are 8×10^{-3} km^{-1} and 1.5×10^{-5} km^{-1}, respectively. Substituting these values into (7), we obtain

$$\Delta\phi = 3.62 \times 10^3\Delta\xi - 1.93 \times 10^6\Delta\eta, \tag{8}$$

where $\Delta\phi$ is in units of degrees latitude and $\Delta\xi$ and $\Delta\eta$ are in units of km^{-1}.

Bryson (1973) has pointed out that the data for the ITCZ in Nigeria (Ilesanmi, 1971) is well correlated with the movement of the subtropical high in the eastern Atlantic Ocean with an amplification factor for the ITCZ movement of ~2.5, in agreement with the results of Beer *et al.* (1977) for the ITCZ in Ghana. Using this amplification factor in Eqs. (8) yields

$$\Delta\lambda_i = 9.1 \times 10^3\Delta\xi - 4.8 \times 10^6\Delta\eta_i, \tag{9}$$

where $\Delta\lambda$ is the expected change in the latitude of the ITCZ for given changes $\Delta\xi$ and $\Delta\eta$. The subscript $i = 0, 1$ corresponds to the two levels at which the meridional temperature gradient is measured as described below Eq. (2).

The values of $\Delta\xi$ and $\Delta\eta$ in Fig. 1 are used to calculate $\Delta\lambda$ in (9). Since $\Delta\xi$ and $\Delta\eta$ are 3-year running means normalized to zero, the resulting $\Delta\lambda$ values are similarly smoothed and normalized. The values of $\Delta\xi$ and $\Delta\eta$ are obtained using temperature data from both the Eastern and Western Hemispheres, as well as the global average. Therefore, we are able to obtain expected movement of the

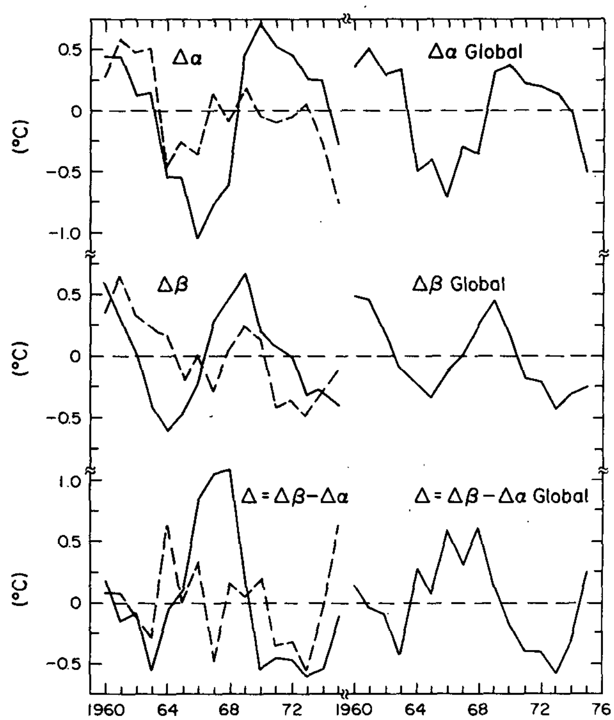

FIG. 3. Southern Hemisphere tropics-south polar temperature gradients as the 500 mb level: Southern Hemisphere summer ($\Delta\alpha$) and winter ($\Delta\beta$) gradients (summer and winter periods as in Fig. 2). In the left-hand side of the figure, the dashed and solid curves are as in Fig. 1. Also, shown is Δ, the summer-winter changes in temperature gradient.

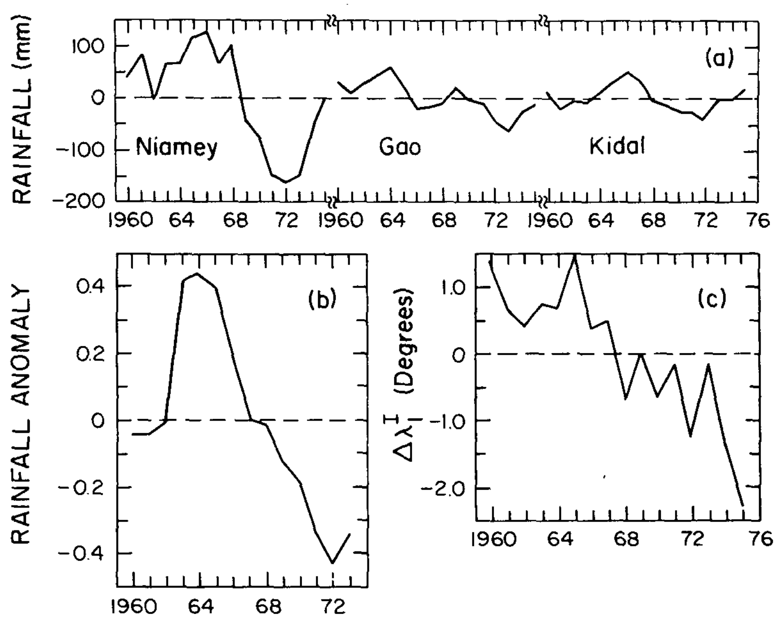

FIG. 4. (a) Annual rainfall for Niamey, Gao and Kidal; (b) rainfall anomaly index (Kraus, 1977); (c) predicted movement of the ITCZ using Model I [Eq. (13)] with Eastern Hemisphere temperature data and meridional temperature gradients at the ~500 mb level.

ITCZ from temperature gradients in the Eastern and Western Hemispheres separately. This represents a departure from the approach of model I where it was assumed that the movement of the West African ITCZ was essentially controlled by the Azores high in the eastern Atlantic Ocean. This would point to temperature gradients in a part of the Western Hemisphere alone as controlling factors in his model. However, since the data are available, we test the $\Delta\lambda$ values obtained using gradients from both hemispheres. A further justification for using Eastern as well as Western Hemisphere data is that a substantial portion of the Sahel is to the east of the 0° longitude.

Comparisons of the predictions of Eq. (9) will be made with rainfall data from stations at three representative latitudes in the Sahel: Niamey, Gao and Kidal at latitudes 13.5, 16.3 and 18.4°N, respectively. Since rainfall at a given station in the Sahel can be quite variable and not necessarily representative of the rainfall trend in the entire region, we also compare the predicted ITCZ movement to the rainfall anomaly index calculated by Kraus (1977) from 26 to 32 stations in the Sahel (depending on the year). Other rainfall trend indices for the Sahel are available (Winstanley, 1973, 1976; Tanaka *et al.*, 1975; Bunting *et al.*, 1976; Nicholson, 1979), but these have been published in graphical form only and are not as accessible as the Kraus index for which numerical values have been tabulated.

The rainfall trends at the three stations and the rainfall anomaly index are shown in Figs. 4a and 4b, where 3-year running means have been taken and the results normalized to zero. The behavior of the rainfall departures in Fig. 4a is reproduced fairly well by the anomaly index in Fig. 4b with a crossover from positive to negative anomalies occurring in approximately 1968 in all cases. However, the differences evident in the three series in Fig. 4a are sufficient to indicate the need for a rainfall index of the type obtained by Kraus.

The correlation coefficients between the values of $\Delta\lambda$ obtained from Eq. (9) and the data in Figs. 4a and 4b are given in Table 3.

Only positive correlation coefficients are of interest since northward movement of the ITCZ should cause increased rainfall to the Sahel. For 95% significance, the correlation coefficient must exceed ~0.5 for the 16 data pairs being compared. The results in Table 3 show that significant correlation is achieved only in the case when Eastern Hemisphere data is used to calculate $\Delta\lambda_1$ and the input meridional temperature gradients are those at the surface–100 mb level. The smoothed and normalized values of $\Delta\lambda_1$ using Eastern Hemisphere data are shown in Fig. 4c. The significant correlation between $\Delta\lambda_1$ and the rainfall anomaly index is obtained mainly because $\Delta\lambda_1$ crosses over from positive to negative values in approximately the same year as does the rainfall data. The precise shape of $\Delta\lambda_1$, with its rapid fluctuations in spite of the smoothing of 3-year running means, differs substantially from the shape of the rainfall anomaly index. In fact, one should presumably demand higher significance than 95% for the correlation coefficients because of the smoothing, although

TABLE 3. Correlation coefficients between the predicted movement of the ITCZ, $\Delta\lambda_i$ [model I, Eq. (9)], and rainfall data from three Sahelian stations and the rainfall anomaly index of Kraus (1977). The rainfall data are for the years 1960–75 (through 1973 for the rainfall anomaly data). Positive correlation coefficients with significance > 95% are in italics.

ITCZ movement	Correlation coefficients: Rainfall anomaly	Niamey	Gao	Kidal
EASTERN HEMISPHERE DATA				
$\Delta\lambda_0$	0.08	0.21	0.05	0.43
$\Delta\lambda_1$	*0.70*	*0.51*	*0.60*	0.31
WESTERN HEMISPHERE DATA				
$\Delta\lambda_1$	−0.11	0.27	0.22	−0.07
$\Delta\lambda_1$	−0.16	0.20	0.27	−0.17
GLOBAL DATA				
$\Delta\lambda_0$	−0.08	0.30	0.22	0.05
$\Delta\lambda_1$	0.14	0.39	0.48	0.01

the correlation of 0.70 between $\Delta\lambda_1$ and the rainfall anomaly index is significant at a level > 99%.

A similar analysis has been carried out using a different model for the subtropical high latitude as a function of ξ and η (Greenhut, 1977). Here, Eq. (6) is used as a starting point, but the ϕ dependence of ξ and η, as derived from the data of Peixoto (1958, 1960) is taken into account. Correlation coefficients analogous to those in Table 3 have been obtained for this model and no significant correlations are observed. We conclude that this model totally fails to describe the rainfall variation in the Sahel during the period 1960–75.

The ITCZ index of model I shows significant correlation with rainfall data from the Sahel only when Eastern Hemisphere data is used. Since this is a departure from the point of view taken by Bryson, model I is not fully confirmed by the data. Nonetheless, it is of interest to see what forcing of rainfall by ITCZ motion is obtained in this model and compare with the results of Fig. 6 in the Appendix, where the ITCZ rainfall model of Ilesanmi (1971) is used to calculate the expected change in rainfall ΔR for given changes in the mean location of the ITCZ, $\Delta\lambda_a$, and for given changes in amplitude of motion of the ITCZ, $\Delta\lambda_b$. A linear regression analysis comparing $\Delta\lambda_1$ using Eastern Hemisphere data with rainfall at Niamey and Gao gives values for $\Delta R/\Delta\lambda$ of 77 ± 35 mm rainfall deg^{-1} of latitude and 29 ± 11 mm rainfall deg^{-1} of latitude, respectively. Since the change in rainfall is due to both $\Delta\lambda_a$ and $\Delta\lambda_b$,

$$\Delta R = \frac{\partial R}{\partial \lambda_a}\Delta\lambda_a + \frac{\partial R}{\partial \lambda_b}\Delta\lambda_b$$

or

$$\frac{\Delta R}{\Delta\lambda} \approx \frac{\partial R}{\partial \lambda_a} + \frac{\Delta\lambda_b}{\Delta\lambda_a}\frac{\partial R}{\partial \lambda_b}. \tag{10}$$

There is some evidence that an increase in the mean location of the ITCZ causes a decrease in the amplitude of its motion (Beer *et al.*, 1977). If we make the simplifying assumption that these two effects are proportional to one another, then

$$\frac{\Delta\lambda_b}{\Delta\lambda_a} \approx -k \tag{11}$$

and substituting this into (10)

$$\frac{\Delta R}{\Delta\lambda} \approx \frac{\partial R}{\partial \lambda_a} - k\frac{\partial R}{\partial \lambda_b}. \tag{12}$$

From Fig. 6, for Niamey (latitude 13.5°N),

$$\frac{\partial R}{\partial \lambda_a} = 160 \text{ mm deg}^{-1}, \quad \frac{\partial R}{\partial \lambda_b} = 107 \text{ mm deg}^{-1}$$

and for Gao (latitude 16.3°N),

$$\frac{\partial R}{\partial \lambda_a} = 115 \text{ mm deg}^{-1}, \quad \frac{\partial R}{\partial \lambda_b} = 93 \text{ mm deg}^{-1}.$$

Substituting these values into Eq. (12) and using the linear regression values obtained above for $\Delta R/\Delta\lambda$, we obtain $k = 0.76 \pm 0.33$ and $k = 0.92 \pm 0.12$ for Niamey and Gao, respectively. Since both values of k are positive, this is additional evidence that northward displacement of the mean position of the ITCZ causes a decrease in the amplitude of its annual movement. In addition, the proportionality between these two effects seems to be fairly large, i.e., close to one, indicating that the maximum latitude of the ITCZ remains fairly constant independent of the motion of the mean latitude.

As an additional comparison of the Northern Hemisphere temperature data with Sahelian rainfall, we have calculated the correlation coefficients between the temperature gradient data in Fig. 1 and the rainfall data in Figs. 4a and 4b. The results are shown in Table 4, where correlations with significance > 95% are in italics. The significant correlations obtained in Table 3 between $\Delta\lambda_1$ and rainfall seem to be due to fairly significant correlation between the vertical lapse rate parameter, $\Delta\xi$, obtained using Eastern Hemisphere data, and Sahel rainfall. In Fig. 1, this parameter is seen to cross over from positive to negative values in approximately the same year as do the rainfall data. However, $\Delta\xi$ for the Eastern Hemisphere exhibits rapid fluctuations which are not evident in the rainfall data of Figs. 4a and 4b.

The overall results in Table 4 indicate that it is the meridional temperature gradients $\Delta\eta$ which are well correlated with Sahelian rainfall. This is particularly true if temperature data from the Western Hemisphere are used, although fairly significant correlation is obtained when global averages are used for the meridional temperature gradient index $\Delta\eta_1$ at the surface–100 mb level. These results parallel those of Korff and Flohn (1969) who obtain the following linear relation between ϕ, the latitude of the subtropical high, and ΔT, the equator-pole temperature gradient (analogous to $TT_i - TN_i$ in our notation)

$$\cot\phi = 0.0245\Delta T + 0.7245. \tag{13}$$

Since

$$\Delta(\cot\phi) = \frac{\partial(\cot\phi)}{\partial\phi}\Delta\phi = -\csc^2\phi\Delta\phi \approx -3.0\Delta\phi,$$

where we have used $\phi \approx 35°$ for the approximate mean latitude of the subtropical high, the slope in Eq. (13) would be $0.0245/(-3.0) = -0.0081$ if one plotted ϕ (in rad) vs ΔT, instead of $\cot\phi$ vs ΔT.

It is of interest to compare this slope with the values obtained in a linear regression analysis of $\Delta\eta$ versus the rainfall anomaly index of Kraus in the cases where significant correlation coefficients are obtained (Table 4). Letting $a_K = m(\Delta\eta \times 10^7)$, where a_K is the rainfall anomaly index, we find

$$m = \begin{cases} 0.25 \pm 0.09; & \Delta\eta_0,\ \text{Eastern Hemisphere} \\ -0.20 \pm 0.07; & \Delta\eta_0,\ \text{Western Hemisphere} \\ -0.23 \pm 0.07; & \Delta\eta_1,\ \text{Western Hemisphere} \\ -0.32 \pm 0.14; & \Delta\eta_1,\ \text{global,} \end{cases} \tag{14}$$

where m is in units of kilometers. The rainfall anomaly index is the sum of rainfall deviations from the mean divided by standard deviations (Kraus, 1977). Therefore,

$$a_K \sim \frac{\Delta R}{\sigma} = \frac{1}{\sigma}\frac{\partial R}{\partial\lambda}\Delta\lambda = \frac{1}{\sigma}\frac{\partial R}{\partial\lambda}\left(\frac{\Delta\lambda}{\Delta\phi}\right)\Delta\phi$$

and inverting, we obtain

$$\Delta\phi \approx a_K\sigma\left(\frac{\partial R}{\partial\lambda}\right)^{-1}\frac{\Delta\phi}{\Delta\lambda}. \tag{15}$$

As discussed previously, Ilesanmi (1971) and Beer *et al.* (1977) have found that the movement of the ITCZ is correlated with that of the subtropical high with an amplification of ~2.5 so that $\Delta\phi/\Delta\lambda \sim 0.4$. From Fig. 5, a typical value for σ for stations in the Sahel is ~100 mm and from Fig. 6, $\partial R/\partial\lambda \approx 125$ mm deg^{-1} latitude. Putting these values into Eq. (20), we obtain

TABLE 4. Correlation coefficients between the temperature gradient indices in Fig. 1 and the rainfall data of Figs. 4a and 4b. Correlation coefficients with significance > 95% are in italics.

Temperature gradient indices	Correlation coefficients: Rainfall anomaly	Niamey	Gao	Kidal
EASTERN HEMISPHERE DATA				
$\Delta\xi$	*0.63*	0.45	*0.52*	0.30
$\Delta\eta_0$	*0.65*	0.36	*0.57*	−0.02
$\Delta\eta_1$	−0.27	−0.33	−0.42	−0.11
WESTERN HEMISPHERE DATA				
$\Delta\xi$	−0.39	−0.05	0.01	−0.28
$\Delta\eta_0$	*−0.67*	*−0.87*	*−0.60*	−0.47
$\Delta\eta_1$	*−0.68*	*−0.69*	*−0.70*	−0.35
GLOBAL DATA				
$\Delta\xi$	−0.07	0.20	0.25	−0.07
$\Delta\eta_0$	−0.13	−0.48	−0.04	−0.45
$\Delta\eta_1$	*−0.55*	*−0.59*	*−0.64*	−0.28

$$\Delta\phi \approx 0.0056a_K, \tag{16}$$

where $\Delta\phi$ is in radians so that a direct comparison can be made with the results of Korff and Flohn. From Eqs. (2) and (3)

$$\Delta\eta_i = \frac{1}{d_\eta T_i}(TT_i - TN_i) = 1.5 \times 10^{-4}\left(\frac{TT_i - TN_i}{T_i}\right),$$

so that we have

$$a_K = m(\Delta\eta_i \times 10^7) = 1500\frac{m}{T_i}(TT_i - TN_i). \tag{17}$$

Substituting (17) into (16) gives

$$\Delta\phi \approx 8.4\frac{m}{T_i}(TT_i - TN_i) = 8.4\frac{m}{T_i}\Delta T, \tag{18}$$

where $T_i = 300$ K (250 K) for the surface level (surface–100 mb level). Using the values of m in (14), we obtain

$$\Delta\phi \approx \begin{cases} (0.0070 \pm 0.0025)\Delta T; & \Delta\eta_0,\ \text{Eastern Hemisphere} \\ -(0.0056 \pm 0.0020)\Delta T; & \Delta\eta_0,\ \text{Western Hemisphere} \\ -(0.0077 \pm 0.0023)\Delta T; & \Delta\eta_1,\ \text{Western Hemisphere} \\ -(0.0108 \pm 0.0047)\Delta T; & \Delta\eta_1,\ \text{global.} \end{cases} \tag{19}$$

Except for the value obtained using Eastern Hemisphere data, these results agree quite well with the slope of −0.0081 obtained in the analysis of Korff and Flohn. These authors find that in order to obtain agreement with model I with a fixed vertical lapse rate, the value of the lapse rate should be $\sim -7°C$ km^{-1} [see Fig. 3 of Korff and Flohn (1969)]. The results obtained in (19) above are based on a value of ξ equal to 8×10^{-3} km^{-1}. Greenhut (1977) has shown that

$$\frac{\partial T}{\partial z} \approx \frac{T}{2}\left[\xi + 2\left(1 - \frac{1}{\gamma}\right)\frac{1}{p}\frac{\partial p}{\partial z} + C\right],$$

where $\gamma = 1.4$ and $C = 0.030$ km^{-1}. Taking $\partial p/\partial z \approx -70$ mb km^{-1} at $\sim$500 mb, we obtain $\partial T/\partial z \approx -5°C$ km^{-1}, in rough agreement with the value obtained by Korff and Flohn.

The linear regression analysis associated with the significant correlations obtained in Table 4 for rainfall at Niamey and Gao makes it possible to determine the sensitivity of rainfall at these stations to changes in meridional temperature gradients. If we write

$$\Delta R = m(\Delta\eta \times 10^7), \tag{20}$$

then average values of m for Niamey and Gao are -72 ± 20 mm km^{-1} and -25 ± 8 mm km^{-1}, respectively. Since rainfall is positively correlated with the movement of the subtropical high, the negative sign in these coefficients is in agreement with the behavior of model I with $\Delta\xi = 0$ [see Eq. (7)]. Using Eqs. (2), (3) and (20),

$$\Delta R \approx 5.5 m \Delta T, \tag{21}$$

where ΔT is the change in the Northern Hemisphere equator-pole temperature difference. Inserting the values of m obtained above

$$\Delta R \approx \begin{cases} -(400 \pm 110)\Delta T & \text{[Niamey]} \\ -(140 \pm 40\Delta T & \text{[Gao]}, \end{cases} \tag{22}$$

where ΔT is in units of degrees Celsius and ΔR is in units of millimeters of annual rainfall. Thus, the general increase in values of $\Delta\eta$ in Fig. 1 from 1960 to 1975 by $\sim 4 \times 10^{-7}$ km^{-1}, which is equivalent to an increase in the equator-pole temperature difference of $\sim$0.7°C, is related to the decline in annual rainfall of $\sim$280 and $\sim$100 mm at Niamey and Gao, respectively, according to (22). This is in agreement with the observed decline in rainfall during this period at these stations as shown in Fig. 4a.

4. Southern Hemisphere model

Kraus (1977) has proposed a model (model II) for ITCZ motion in West Africa which depends on upper air temperature gradients in the Southern Hemisphere. It is conjectured that reduced northward movement of the ITCZ in the Northern Hemisphere summer, and consequent reduced rainfall in the Sahel, is associated with a decreased demand for energy transport across the equator to the Southern Hemisphere. This reduced demand is a manifestation of a decrease in meridional baroclinicity which can be measured by a reduction in the equator-pole temperature difference at 500–700 mb in the Southern Hemisphere. At least two points of view are taken in this model. One is that annual values of Southern Hemisphere equator-pole temperature gradients for a given season, in particular, the southern winter which corresponds to the furthest northward advance of the ITCZ, are directly related to Sahelian rainfall. Another is that it is the change in equator-pole temperature gradient from the previous southern summer to the southern winter corresponding to maximum northward motion of the ITCZ that is related to rainfall in the Sahel.

The model has been tested in two ways (Kraus, 1977). One is by observing the 500 mb height anomalies and the 700 mb temperature anomalies for both the earlier southern summer and later southern winter in 1972 for stations between 30°S and the equator and stations in the antarctic. The year 1972 was chosen since it was a year of severe drought in the Sahel. The other test was to compare 500 mb height anomalies in both the southern tropics and Antarctica for the periods 1958–64 and 1968–74. In both cases, the model appears to be supported by the data (Kraus, 1977). An excess of negative over positive 500 mb height anomalies (and 700 mb temperature anomalies) was found for stations in the southern tropics and vice versa for stations in Antarctica for 1972. In the southern tropics, an excess of positive 500 mb height anomalies was found in the period 1958–64, changing to an excess of negative anomalies for the period 1968–74. An opposite change was found for the 500 mb height anomalies in the antarctic.

The data in Fig. 2 are not in agreement with the above results. For example, although the south polar temperature anomaly is positive in the Southern Hemisphere winter of 1972 for both Eastern and Western Hemisphere data, the south polar temperature anomaly is essentially zero during the previous winter. Since the temperature departures in Fig. 2 are based on means for the period 1960–75, the zero anomaly obtained for the south polar summer in 1972 may not be in disagreement with Kraus since the periods over which his anomalies are calculated are presumably different. In any event, the temperature trend for the south polar summer shown in Fig. 2 (SS, global) indicates that 1972 was probably a year of transition from negative to positive anomalies.

A greater difference between the data used by Kraus to test model II and the values in Fig. 2 occurs for the southern tropics. For the Eastern Hemisphere, the data in Fig. 2 show little departure from the mean for 1972. For the Western Hemisphere, however, the departures are strongly positive in 1972 for both the Southern Hemisphere summer and winter. In addition, these positive departures are preceded and followed by similar positive departures in the years before and after 1972. In fact, if one takes the periods 1960–64 and 1968–74, roughly corresponding to the two periods used in Kraus' test of model II, then the southern tropics data of Fig. 2 (ST and WT, global) show negative anomalies for the earlier period and positive anomalies for the later period, in disagreement with the data in Table 9 of Kraus (1977).

A more stringent test of the model is to compare the tropics-polar temperature gradients, $\Delta\alpha$ and $\Delta\beta$ in Fig. 3, with the rainfall anomaly index in Fig. 4b. The correlation coefficients are given in Table 5, where correlations with significance > 95% are in italics. No significant correlation is obtained except for the Southern Hemisphere summer gradient when Western Hemisphere temperature data is used. The temperature data in Fig. 2 therefore do not support the point of view in this model that the tropics-polar temperature gradient is related to Sahelian rainfall, particularly since the correlation was suppose to be most strong for the Southern Hemisphere winter.

The other point of view in the model is tested by comparing Δ, the change in tropics-polar temperature gradient from the previous summer to the following Southern Hemisphere winter, shown in Fig. 3, with the rainfall anomaly index of Fig. 4b. The correlation coefficients are given in Table 5. Significant correlation is obtained with the Eastern Hemisphere data at the 95% level which is probably not high enough since both time series have been smoothed. In addition, the rapid fluctuations in the Eastern Hemisphere values of Δ in Fig. 3 are not present in the time series for the rainfall anomaly index of Fig. 4b.

The time series for the globally averaged values of Δ in Fig. 3 does resemble the shape of Fig. 4b. The reason that a correlation coefficient of only 0.44 is obtained is that the crossover from positive to negative values occurs in approximately 1969 for Δ, whereas the crossover is in 1968 for the rainfall series. If correlation is measured between Δ lagged by one year behind the rainfall anomaly index, then correlation coefficients of 0.74, 0.63 and 0.59 are obtained (significant at the 99, 98 and 97% level) for Δ-global, Δ-Eastern Hemisphere and Δ-Western Hemisphere data, respectively. These high correlations are an indication that the movement of the ITCZ in the Northern Hemisphere summer influences the change of the tropics-polar temperature gradient in the Southern Hemisphere during the following seasons, presumably by determining the amount of energy transport across the equator. Larger northward movement of the ITCZ, and consequent higher rainfall in the Sahel implies larger area of energy collection and, therefore, potentially larger amounts of energy transport to the Southern Hemisphere. This larger energy transport produces an increase in the change in southern tropics-polar temperature gradient in the following seasons, i.e., with a lag of 0.5–1 year. The fact that the 1-year lag correlation coefficients are positive is in agreement with this sequence of events.

TABLE 5. Correlation coefficients between the Southern Hemisphere temperature gradients of Fig. 3 and the rainfall anomaly index of Fig. 4b. Correlation coefficients with significance greater than 95% are in italics.

Temperature gradients	Correlation coefficients rainfall anomaly
EASTERN HEMISPHERE DATA	
$\Delta\alpha$	−0.14
$\Delta\beta$	0.37
Δ	*0.53*
WESTERN HEMISPHERE DATA	
$\Delta\alpha$	*−0.60*
$\Delta\beta$	−0.49
Δ	0.23
GLOBAL AVERAGE	
$\Delta\alpha$	−0.49
$\Delta\beta$	−0.12
Δ	0.44

5. Conclusions

We have found that using the temperature departure data of Angell and Korshover (1978) in unsmoothed form as supplied by J. K. Angell (private communication), the Northern Hemisphere models that relate horizontal and vertical temperature gradients to predicted movement of the ITCZ (Bryson, 1973, 1974; Greenhut, 1977) do not correlate well with the observed rainfall in the Sahel over the period 1960–75 (Table 3). When model I (Bryson, 1973, 1974) is used with constant vertical lapse rate, however, as was done by Korff and Flohn (1969) in their study of the motion of the subtropical high, then good correlation is achieved (Table 4), particularly if Western Hemisphere data is used to obtain the meridional temperature gradients. Thus, there is strong evidence that the Northern Hemisphere meridional temperature gradient from tropics to north extratropics is directly related to ITCZ motion and rainfall in the Sahel. Since a similar connection has already been made between meridional temperature gradients and the subtropical high by Korff and Flohn, the ITCZ, Sahel rainfall and the subtropical high appear to be mutually interrelated. Evidence for this interrelationship has been found previously by Beer *et al.* (1977) in their investigation of rainfall and the ITCZ in Ghana.

The model relating Southern Hemisphere temperature gradients to Sahel rainfall (Kraus, 1977) also generally fails to yield correlation coefficients of high significance (Table 5). This is true not only for temperature gradients obtained in both the southern summer and winter, but also for the change in gradient between these two seasons, the latter being a measure of the change in baroclinicity in the Southern Hemisphere which may be produced by changes in cross-equatorial energy transport. However, highly significant correlation is obtained between Sahelian rainfall and the change in the Southern Hemisphere temperature gradient when the latter lags by one year. This is evidence that the northward motion of the ITCZ influences energy transport to the Southern Hemisphere with a lag of a few seasons.

Acknowledgments. This work was done while the author was supported by a grant from the National Science Foundation under the Science Faculty Professional Development Program. It would not have been possible without the assistance of J. K. Angell who supplied the unsmoothed temperature data used in the analysis.

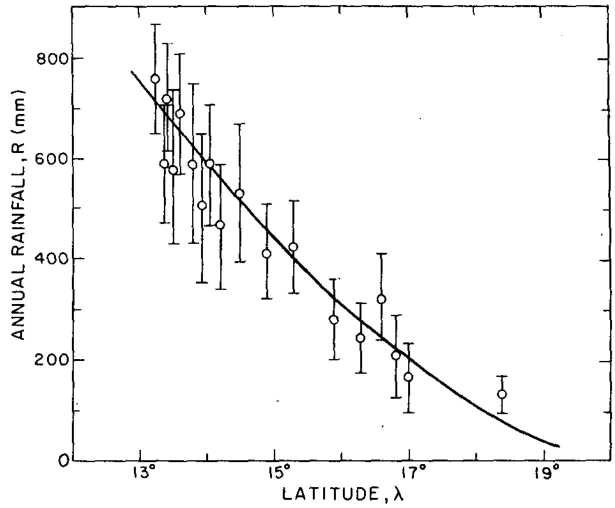

FIG. 5. Annual rainfall R as a function of latitude λ in the Sahel according to the rainfall model of Eq. (A5). The data points and standard deviations are average annual rainfall for 18 stations in Niger, Mali and Upper Volta.

APPENDIX

A Simple Rainfall Model for the Sahel

In the following model, we assume that the yearly movement of the latitude of the ITCZ, λ_{ITCZ}, is sinusoidal, i.e.,

$$\lambda_{\mathrm{ITCZ}} = \lambda_a + \lambda_b \cos(\omega t + a), \tag{A1}$$

where the frequency ω corresponds to a period of 12 months. This assumption is borne out, at least approximately, by the data from Ghana (Beer *et al.*, 1977), where λ_{ITCZ} is seen to vary from $\sim$6–20°, i.e., $\lambda_a \approx 13°$ and $\lambda_b \approx 7°$ in Eq. (A1).

A second assumption is that the rainfall rate increases linearly with latitude λ to the south of the ITCZ. The model of Ilesanmi (1971) is in approximate agreement with this for latitudes as far as $\sim$9° south of the ITCZ, as long as the effect of coastal rainfall is not a factor, which is the case in the Sahel. We, therefore, have

$$\frac{dR}{dt} = K(\lambda_{\mathrm{ITCZ}} - \lambda)$$

$$= K[\lambda_a - \lambda + \lambda_b \cos(\omega t + a)], \tag{A2}$$

where R is the amount of rainfall and, from the model of Ilesanmi (1971), $K \approx 28$ mm (month-degree)$^{-1}$. This slope also agrees approximately with the August precipitation curves given by Tanaka *et al.* (1975) for Sahelian stations along approximately 0° longitude. The linear relationship (A2) implies that the rainfall rate is zero north of the ITCZ which is an approximation. However, for stations sufficiently far south of the northern most reaches of the ITCZ, the small rainfall rate north of the ITCZ latitude will have little effect on our results.

Since the rainfall rate is assumed to be zero north of the ITCZ latitude, rainfall will occur at a given latitude λ only when the ITCZ is north of it. The times when the ITCZ crosses latitude λ is given by solutions to the equation $\lambda = \lambda_{\mathrm{ITCZ}}$, where λ_{ITCZ} is given by Eq. (A1). Solving for t, we have

$$t_{1,2} = \frac{1}{\omega}\left[\cos^{-1}\left(\frac{\lambda - \lambda_a}{\lambda_b}\right) - a\right]. \tag{A3}$$

From (A2), the total rainfall at latitude λ is

$$R = \int_{t_1}^{t_2} K[\lambda_a - \lambda + \lambda_b \cos(\omega t + a)]dt. \tag{A4}$$

Doing the integral with the limits (A3) gives the result

$$R = \frac{2K}{\omega}\left[[\lambda_b^2 - (\lambda - \lambda_a)^2]^{1/2} - (\lambda - \lambda_a)\cos^{-1}\left(\frac{\lambda - \lambda_a}{\lambda_b}\right)\right], \tag{A5}$$

where R is the total annual rainfall at a latitude λ. The function in (A5) is plotted in Fig. 5 along with average annual rainfall data for 18 stations in Niger, Mali and Upper Volta. The data are from the archives at the National Center for Atmospheric Research and are averages and standard deviations over 20–32 years depending on the station. The agreement between data and Eq. (A5) is quite good.

We can now use Eq. (A5) to determine the change in annual rainfall at a given latitude in the Sahel due to a change in the average location of the ITCZ,

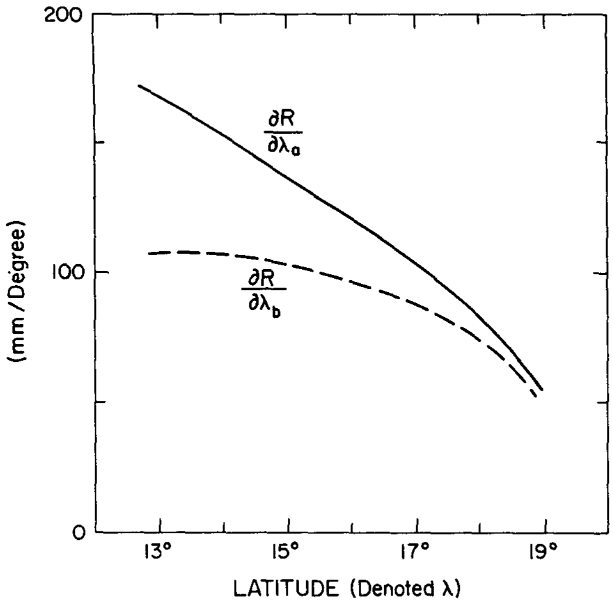

FIG. 6. Rate of change of annual rainfall in the Sahel as a function of latitude due to a change in the average location of the ITCZ [$\partial R/\partial\lambda_a$, Eq. (A6)] and due to change in the amplitude of annual motion of the ITCZ [$\partial R/\partial\lambda_b$, Eq. (A7)].

λ_a, or due to a change in the amplitude of oscillation of the ITCZ, λ_b. Taking derivatives of (A5)

$$\frac{\partial R}{\partial\lambda_a} = \frac{2K}{\omega}\cos^{-1}\left(\frac{\lambda - \lambda_a}{\lambda_b}\right), \tag{A6}$$

$$\frac{\partial R}{\partial\lambda_b} = \frac{2K}{\omega\lambda_b}[\lambda_b^2 - (\lambda - \lambda_a)^2]^{1/2}. \tag{A7}$$

The units of these expressions are, for instance, millimeters of rainfall per degree latitude change in λ_a or λ_b. Eqs. (A6) and (A7) are plotted in Fig. 6 as a function of λ. The rate of change of annual rainfall for a given change in either the average latitude of the ITCZ or in the amplitude of its annual oscillation can be read off the curves for a given latitude in the Sahel. The accuracy of this result is expected to decrease as one goes to higher latitudes since the model assumes zero rainfall rate north of the location of the ITCZ while the actual average rainfall rates there could be as high as ~10 mm $(\text{month})^{-1}$ (Ilesanmi, 1971).

REFERENCES

Angell, J. K., and J. Korshover, 1977: Estimate of the global change in temperature, surface to 100 mb, between 1958 and 1975. *Mon. Wea. Rev.*, **105**, 375–385.

——, and ——, 1978: Global temperature variation, surface–100 mb: An update into 1977. *Mon. Wea. Rev.*, **106**, 755–770.

Beer, T., G. K. Greenhut and S. E. Tandoh, 1977: Relations between the Z criterion for the subtropical high, Hadley cell parameters and the rainfall in Northern Ghana. *Mon. Wea. Rev.*, **105**, 849–855.

Bryson, R. A., 1973: Drought in Sahelia, who or what is to blame? *Ecologist*, **3**, 366–371.

——, 1974: A perspective on climatic change. *Science*, **184**, 753–760.

Bunting, A. H., M. D. Dennett, J. Elston and J. R. Milford, 1976: Rainfall trends in the West African Sahel. *Quart. J. Roy. Meteor. Soc.*, **102**, 59–64.

Flohn, H., 1964: Grundfragen der Palaeoklimatologie im Lichte einer theoretischen Klimatologie. *Geol. Rundsch.*, **54**, 504–515.

——, 1965: Probleme der theoretischen Klimatologie. *Naturwiss. Rundsch.*, **18**, 385–392.

Greenhut, G. K., 1977: A new criterion for locating the subtropical high in West Africa. *J. Appl. Meteor.*, **16**, 727–734.

Ilesanmi, O. O., 1971: An empirical formulation on an ITD rainfall model for the tropics: A case study of Nigeria. *J. Appl. Meteor.*, **10**, 882–891.

Korff, H. C., and H. Flohn, 1969: Zusammenhang zwischen dem Temperaturgefälle Äquator-Pol und den plaetarischen Luftdruckgürteln. *Ann. Meteor.* (N.F.), **4**, 163–164.

Kraus, E. B., 1977: Subtropical droughts and cross-equatorial energy transports. *Mon. Wea. Rev.*, **105**, 1009–1018.

Mitchell, J. M., 1976: An overview of climatic variability and its causal mechanisms. *Quat. Res.*, **6**, 481–493.

Nicholson, S. E., 1979: Revised rainfall series for the West African subtropics. *Mon. Wea. Rev.*, **107**, 620–623.

Peixoto, J. P., 1958: Hemispheric humidity conditions during the year 1950. Sci. Rep. No. 3, Contract AF 19(604)-2242, Rep. No. AFCRC-TN-58-609, Dept. of Meteorology, MIT, 142 pp.

——, 1960: Hemispheric temperature conditions during the year 1950. Sci. Rep. No. 4, Contract No. AF 19(604)-2242, Rep. No. AFCRL-TN-60-818, Dept. of Meteorology, MIT, 211 pp. [NTIS AD 250-698].

Phillips, N. A., 1954: Energy transformations and meridional circulations associated with simple baroclinic waves in a two-level quasi-geostropic model. *Tellus*, **6**, 273–286.

Smagorinsky, J., 1963: General circulation experiments with the primitive equations. *Mon. Wea. Rev.*, **91**, 99–164.

Tanaka, M., B. C. Weare, A. R. Navato, and R. E. Newell, 1975: Recent African rainfall patterns. *Nature*, **255**, 201–203.

Winstanley, D., 1973: Recent rainfall trends in Africa, the Middle East and India. *Nature*, **243**, 464–465.

——, 1976: Climatic change and the future of the Sahel. *The Politics of Natural Disaster*, M. H. Glantz, Ed., Praeger Publ., 340 pp.